HHS Public Access

Author manuscript

Int J Radiat Oncol Biol Phys. Author manuscript; available in PMC 2020 August 23.

Published in final edited form as:

Int J Radiat Oncol Biol Phys. 2019 May 01; 104(1): 177–187. doi:10.1016/j.ijrobp.2019.01.073.

A Current Review of Spatial Fractionation: Back to the Future?

Cole Billena, BS, **Atif J. Khan, MD**

Department of Radiation Oncology, Memorial Sloan Kettering Cancer Center, New York, New York

Abstract

Spatially fractionated radiation therapy represents a significant departure from canonical thinking in radiation oncology despite having origins in the early 1900s. The original and most common implementation of spatially fractionated radiation therapy uses commercially available blocks or multileaf collimators to deliver a nonconfluent, sieve-like pattern of radiation to the target volume in a nonuniform dose distribution. Dosimetrically, this is parameterized by the ratio of the valley dose in cold spots to the peak dose in hot spots, or the valley-to-peak dose ratio. The radiobiologic mechanisms are postulated to involve radiation-induced bystander effects, microvascular alterations, and/or immunomodulation. Current indications include bulky or locally advanced disease that would not be amenable to conventional radiation or that has proved refractory to chemoradiation. Early-phase clinical trials have shown remarkable success, with some response rates >90% and minimal toxicity. This has promoted technological developments in 3-dimensional formats (LATTICE), micron-size beams (microbeam), and proton arrays. Nevertheless, more clinical and biological data are needed to specify ideal dosimetry parameters and to formulate robust clinical indications and guidelines for optimal standardized care.

Introduction

Since the codification of radiotherapy target volume definition by the International Commission on Radiation Units, radiation oncologists have strived to deliver a homogenous dose of radiation to the entire target volume. Any departure from this paradigm would be viewed as heterodoxical by the most charitable of critics and frankly heretical by others. Yet spatially fractionated grid radiation therapy (GRID) has been investigated as a modality for decades and is clearly associated with dramatic responses, often exceeding those expected with homogenous dosing. GRID therapy uses blocks or multileaf collimators (MLCs) to deliver a nonconfluent, sieve-like pattern of radiation to the target volume in a nonuniform dose distribution. There is intentional heterogeneity and high doses within the target but also areas of underdosing. Current advances in radiation therapy technology permit alternative methods of introducing dose heterogeneity within the target volume (3-dimensional lattice therapy, proton grids, microbeams, and flash irradiation). We now also have clearly testable biological hypotheses to explain the empirically observed efficacy of GRID and related modalities. Here we review current literature investigating intentional dose heterogeneity,

Reprint requests to: Atif J. Khan, MD, Department of Radiation Oncology, Memorial Sloan Kettering Cancer Center, 1275 York Ave, New York, NY 10065. Tel: (848) 225-6334; khana7@mskcc.org.

Conflict of interest: none

which we will refer to as spatially fractionated radiation therapy (SFRT). GRID therapy is the first method of SFRT, whereas lattice radiation therapy (LRT) is a 3-dimensional alternative to GRID that involves the deposition of spheres of high-dose radiation therapy within the tumor. Our review is divided into 4 parts: (1) we review the basic terminology of SFRT and the strengths and weaknesses of each method of delivery; (2) we review the clinical data to discern common dosage, response rates, and toxicity profiles; (3) we explore the putative radiobiological mechanisms underpinning spatial fractionation; and (4) we consider future directions of this emerging therapy, briefly touching on new technological advances using new formats and particles.

Current Methods of Delivery

Kohler et al[1] introduced SFRT in 1909, with the intention of treating deep-seated tumors and overcoming the skin toxicities associated with the poorly penetrating orthovoltage x-rays of the time. It was noted that smaller irradiated volume permitted higher dose tolerance, and through spatial fractionation, doses as high as 20 times the conventional doses could be tolerated by the skin.[2,3] However, SFRT was disregarded when deeply penetrating megavoltage linear accelerators rendered the primary objective of the method null.[4] Interest in SFRT would not be renewed until 1990, when Mohiuddin et al demonstrated the feasibility of this technique with bulky and refractory tumors, historically considered to be resistant to standard fractionated radiation therapy.[5,6]

SFRT, in its original form, requires the simple collimation of a broad-based photon beam into pencil beam–shaped, nonconfluent grids to create hexagonal or orthogonal patterns of “hot spots” surrounded by peripheries of nonirradiated tissue (Fig. 1).[7,8] We will refer to this method as GRID and note that it was the original method described by Kohler et al. To date, it is the most commonly reported SFRT dose pattern, with the greatest body of clinical evidence. In GRID therapy, the peak dose refers to the dose along the unblocked beam path, whereas the valley dose refers to the minimum dose from blocked areas resulting from leakage and scatter radiation.[8] The valley-to-peak ratio thereby quantifies the degree of spatial fractionation. Important parameters of the grid include the hole diameter and hole center-to-center spacing.[8] Using Monte Carlo simulations, Gholami et al[9] found that hole sizes in the range of 1 to 1.25 cm and spacing of 1.7 to 1.8 cm optimize therapeutic ratio and normal tissue sparing.

GRID therapy was first delivered using attenuation blocks with regularly spaced apertures that can be mounted onto the linear accelerator head (Fig. 1a).[5] Commercially available compensators are made of Cerrobend (Radiation Products Design, Inc, Albertive, MN) or brass (dot Decimal Inc, Sanford, FL).[10,11] Both are made to order with customizable aperture sizes, center-to-center spacing, and holes that follow beam divergence. The initial Cerrobend block had a 50% open-to-closed field ratio.[5] Evaluation of the Cerrobend block with 1.4-cm hole diameter and 2.1-cm center-to-center spacing demonstrated a valley-to-peak ratio of approximately 20% for 6 MV and 25% to 32% for 18 MV at 10-cm depth in a water phantom.[10] Similarly, the brass block with 1-cm hole diameter and 2-cm center-to-center spacing revealed a valley-to-peak ratio of around 27% for 6 MV and 35% for 18 MV.[11]

To equip more institutions with GRID capability, Ha et al introduced a method of collimation using MLCs that administers beams 2 rows at a time in a step-and-shoot fashion (Fig. 1b).[12,13] The valley-to-peak ratio at 10-cm depth of MLCs with 5 × 5 mm and 10 × 10 mm apertures with 6 MV were 17% and 25%, respectively.[12] The open-to-closed ratio is 31%, less than that of a block.[13] GRID therapy with MLCs gives more flexibility in determining aperture size and center-to-center spacing on a case-by-case basis without having to commission the creation of a new block. Apertures that target organs at risk (OARs) or other critical structures can easily be closed.[13] The major limitation is the length of treatment time, which increases as a factor of the number of segments per step-and-shoot method of delivery.[14] The number of monitor units rises and consequently so does radiation leakage, which may undesirably increase surface doses and valley-to-peak ratios.[11] In a clinical setting, Neuner et al[13] found that MLC-based GRID delivery was comparable to block-based GRID.

Another method involves hybrid collimation using both a block and an MLC, each creating a set of parallel stripes when set perpendicular to one another form a grid.[15] Interestingly, the valley-to-peak ratio is lower along the diagonal axes where the beam is shielded by both the block and the MLC leaves. The valley-to-peak ratio, calculated as the mean valley-to-peak ratio for the different valleys, is 16.2% for 6 MV and 20.5% for 18 MV with 1-cm hole size and 2-cm center-to-center spacing. Although it is unknown whether smaller valley-to-peak ratios in some areas are clinically relevant, this technique reduces the duration of treatment in multisegment plans compared to MLC-based GRID and remains lighter than block-based GRID. Table 1 lists the strengths and weaknesses of the more common modalities.

A novel development, TOMOGRID, uses helical tomotherapy to improve the dose conformity of GRID.[16] Using in-house software, the authors programmed aperture size, center-to-center shaping, aperture shape, grid pattern, and OAR avoidance. Compared to a block-based GRID in a virtual study, TOMOGRID produced similar gross tumor volume (GTV) dose-volume histograms, maximum GTV doses, and valley-to-peak ratios while confining maximal doses within the GTV and away from nearby normal skin and lungs. Similarly, GRID using volumetric modulated arc therapy has been shown to be feasible.[17] Planning a target in a water phantom demonstrated a valley-to-peak ratio of 19%, comparable to the 22% produced by the block control. The therapeutic ratios, calculated using dose profiles and defined as the ratio between surviving cell fractions in normal and tumor cells in irradiated and nonirradiated fields, were 1.25 for volumetric modulated arc therapy versus 1.38 for the block.

Clinical Trials

In 1990, Mohiuddin et al[5] first evaluated the potential of GRID in a pilot study of 22 patients with diverse cancer types, refractory to all conventional therapy, in a palliative care setting. Using a 50% open/50% blocked Cerrobend block in a single unopposed field with a dose range of 10 to 15 Gy, they found an excellent 91% response rate in symptoms, with 5 patients having mild skin and gastrointestinal toxicity and 1 patient having a late small bowel obstruction that required surgical correction. Six patients received prior radiation. Conventional external beam radiation therapy (EBRT) was added to GRID in 14 patients,

and a second GRID treatment was given in 4 patients. The use of these additional treatments makes the incremental utility of GRID difficult to understand, which is a recurring theme in the extant literature of GRID therapy.

In 2 follow-up studies, Mohiuddin et al treated 132 patients total with GRID alone or GRID with EBRT in a palliative care setting with diverse tumors and corroborated overall response rates higher than 90%.[7,18] In both studies, there was 1 reported grade 3 mucositis, and 1 death was attributed to rapid tumor lysis and carotid blowout.[18] Sixteen percent of patients had a history of radiation treatment of the site. GRID alone was given to 31% of patients. GRID doses ≥15 Gy were found to have higher response rates than doses <15 Gy.[7] GRID therapy also had higher complete response rates when complemented with EBRT of at least 40 Gy, compared to EBRT doses less than 40 Gy.[7,18] Squamous cell carcinomas and soft tissue sarcomas were the most responsive cancer types.[7] Notably, 8 patients were treated definitively with GRID followed by surgical resection. All patients responded, with 5 patients achieving a complete response.[18]

Neuner et al[13] compared the clinical outcomes in diverse tumor types with GRID (median, 15 Gy) using Cerrobend block versus MLCs. Of 79 patients, 23% were treated with curative intent; notably, EBRT after GRID was added in approximately 80% of patients. Although MLC-based GRID has an open-to-closed ratio of 31% against the 50% of block, response rates for pain (62% vs 68%), mass effect (62% vs 55%), and other less common complaints were similar between Cerrobend block and MLC, respectively. Grade 3 and 4 adverse reactions, primarily dermatologic, were statistically nonsignificant (17.5% MLC vs 5.1% Cerrobend block) and were noted to be more likely related to the dosing of EBRT because there was no grade 2 to 4 toxicity in patients who received <45 Gy EBRT.

Kudrimoti et al[19] treated 20 bulky, N2 to N3 melanomas (>8-cm diameter) with GRID (median, 15 Gy) and EBRT, finding an overall local control rate of 80%, an overall palliative response rate of 53%, and no toxicities of grade 3 or worse. Five sites were irradiated previously; in these patients, GRID was administered alone.

Mohiuddin et al[20] evaluated GRID in recurrent or unresectable soft tissue sarcomas (median diameter, 13 cm) in 33 patients. Of 44 treatment sites, 4 were treated with GRID only; the rest were given GRID (median dose, 15 Gy) and EBRT. They achieved a 76% response rate, noting an improved 95% response rate among patients who received EBRT >50 Gy. Only 2 patients had acute grade 3 skin toxicities, and treatments delivered to the abdomen and pelvis did not cause significant side effects.

Mohiuddin et al[21] then assessed the tolerability of induction GRID in upfront treatment of large (median, 11.5 cm) extremity soft-tissue sarcoma. Before standard preoperative chemoradiation, patients received 1 fraction of 18 Gy GRID. All 14 patients in the study were free of disease at the time of last follow-up (median, 14 months), and 9 patients had >90% tumor necrosis. Two patients failed to complete the study treatment plan because of grade 3 dermatitis and warranted foot amputation mid-treatment, respectively. Limb salvage surgery in 12 of 13 patients was achieved with negative margins, and postoperative complications included 2 patients with poor wound healing.

There has been considerable research evaluating GRID in the definitive treatment of locally advanced head and neck squamous cell carcinomas. Huhn et al[22] reported the first experience using upfront GRID to treat 27 patients with bulky head and neck tumors. Fourteen patients underwent block-based GRID (median, 15 Gy) followed by EBRT, and 86% had local neck control at 44 months. Another 13 patients underwent GRID, EBRT, and surgery, and the local control rate was 92% after 116 months. Early and late toxicities were acceptable. There were no grade 4 toxicities, and post-surgical complications included only poor wound healing in 3 patients. This study proved the feasibility of adding GRID therapy to current regimens in upfront therapy.

In contrast, Penagaricano et al[23] evaluated the use of MLC-based GRID (20 Gy) with chemotherapy and simultaneous integrated boost intensity modulated radiation therapy (IMRT) in the curative treatment of locally advanced head and neck squamous cell carcinomas (≥6-cm diameter). The local control rate was 79% with 3 recurrences in the treated field; of the 10 patients who had surgery or biopsy of the irradiated tumor, 8 displayed pathologic complete response. Notably, all skin and mucosal toxicities were limited to grade 3 or lower despite co-treatment with chemotherapy and IMRT. There was 1 mortality secondary to a carotid-to-skin fistula.

Edwards et al[24] retrospectively reviewed their experience definitively treating 53 patients with T4/N3 M0 head and neck squamous cell carcinoma using 15-Gy GRID induction immediately followed by conventional EBRT. The local control rate at 3 years was 81%. Adverse effects included 2 late grade 3 to 4 toxicities requiring feeding tubes. Interestingly, the authors noticed a rate of distant metastasis (9% over 3 years) lower than expected with this stage of disease, possibly attributable to an abscopal effect.

In Table 2, we summarize the most important GRID studies reported. Figure 2 demonstrates 2 cases of dramatic responses with GRID therapy.[25,26]

The results of available clinical data on GRID therapy are legitimate grounds for excitement: The response rates appear to be higher than established historical precedent. However, there are also important limitations of the studies described. In most cases, interpretation of these studies is confounded by (1) lack of a control arm; (2) significant heterogeneity in the study population; (3) uncontrolled or inconsistent combination with conventional EBRT; and (4) unclear dose and delivery methods relative to target volumes and OARs. This last point merits further contemplation. GRID therapy is fundamentally a 2-dimensional delivery of dose and hence subject to the physical attenuation of dose as a function of depth. With photon therapy, this means that dose falloff from the maximum dose to any given depth in the target volume is inherently variable and subject to the shape and depth of the target volume (Fig. 3). Put another way, an identical GRID geometry and prescription will deliver wildly different doses to different target volumes (and OARs) depending on the specific anatomical context.

Radiobiology

Spatial fractionation minimizes the toxicity of high-dose radiation by limiting the volume of normal tissue receiving radiation (ie, the dose-volume effect). This allows nearby normal cells to migrate and mediate repair damaged areas.[27,28] Although tumor volume is spared direct physical radiation, SFRT remains clinically effective by leveraging nontarget effects and tumor microenvironment changes.[27] The tumoricidal mechanisms putatively active in nonhomogeneous radiation fields involve signal-mediated effects in the neighborhood of the irradiated tumor (bystander) and in distant sites (abscopal).

Bystander effects

Radiation-induced bystander effects can be defined as the cellular and biological effects of unirradiated cells in response to signals from irradiated cells within a radiation field.[29] Nagasawa and Little first discovered this phenomenon when sister chromatid exchange was induced in 30% of cells when only 1% of cell nuclei were traversed by alpha particles. Transfer of serums from Chernobyl survivors and in vitro cells exposed to radiation demonstrated clastogenic activity in normal cell cultures.[30,31] Further research elucidated the importance of intercellular communication, most notably gap junctions and secreted soluble factors, and the involvement of radical oxygen and nitrogen species and cytokines (eg, IL-6, IL-8, TGFB1, and TNFa) mediating inflammatory pathways.[32–34]

In SFRT, in contrast to the strict definition of bystander, the bystander cells are understood to be the tumor cells located in the valley regions. In preclinical murine models using SFRT, Asur et al[35] found that bystander tumor cells had cell survival rates less than what would be expected with valley doses and had significant overexpression of DNA repair, apoptosis, cell cycle control, heat shock protein, and antioxidant/pro-oxidant genes.[35] Sathishkumar et al[36] found that TNFa, a cytokine associated with tumor killing, was induced from baseline levels in 32% of patients treated with GRID therapy and was correlated with improved clinical response, whereas TGFb, a cytokine putatively associated with tumor burden, decreased in 50% with no correlation to response rates. In lung adenocarcinoma cell lines, Shareef et al[37] reported the induction of TNFa with activation of the NF-KB pathway and upregulation of TRAIL with translocation of pro-apoptotic PAR4 protein into the nucleus. Another study using mice with allogenic Lewis lung carcinoma and treated with 3-dimensional GRID (LATTICE) also found increases in TNFa and TRAIL after partial irradiation, correlating with tumor growth inhibition.[38]

Microvascular changes

Ionizing radiation has been shown to cause endothelial apoptosis through soluble factors, consequently altering tumor microvasculature, which is vital for tumor growth and metastatic evolution.[39] Haimovitz-Friedman et al[40] demonstrated that radiation induces apoptosis in bovine aortic endothelial cells (BAECs) via the hydrolysis of sphingomyelin into ceramide, a second messenger that activates the apoptotic pathway. They observed that radiation induced ceramide production in BAEC, the DNA of BAECs incubated with a ceramide analog exhibited fragmentation indicative of apoptosis, and ceramide returned

radiation-induced apoptotic potential despite the inhibition by activated protein kinase C. Santana et al[41] confirmed in sphingomyelinase knockout murine cells and lymphoblasts from patients with Neimann-Pick disease that the production of ceramide by acid sphingomyelinase (ASMase) is a necessary component in a radiation-induced apoptotic pathway that is independent of P53. Radiation failed to induce apoptosis in these ASMase-deficient cells; yet in the Neimann-Pick disease lymphoblasts, radiation-induced apoptotic potential was restored after viral transduction of ASMase-encoding complementary DNA. With B16F1 melanomas and MCA/129 fibrosarcomas cultivated in an ASMase-deficient murine model, Garcia-Barros et al found that endothelial cells were less likely to undergo apoptosis at baseline and after radiation.[42,43] These tumors had faster growth and increased tumor radioresistence. Other studies noticed that restoration of intracellular ceramide generation via inhibition of downstream ceramide metabolism conferred sensitivity to radiation in human glioma and radioresistant squamous cell carcinoma.[44,45]

Sathishkumar et al[46] measured ceramide and secretory sphingomyelinase (SSMase), a secreted protein product of ASMase that results in endothelial ceramide accumulation and apoptosis, in patients after GRID therapy. In those who responded clinically, 63% and 75% had an increase in SSMase activity and ceramide levels, respectively, whereas those who had no clinical response had no change or a decrease in SSMase activity and ceramide levels. In treatment of 6 dogs with bulky soft-tissue sarcoma, there was no reduction in tumor volume in any of the dogs after GRID, and measured SSMase and TNFa serum levels were all significantly decreased.[47] Serum derived from mice with allogenic Lewis lung carcinoma tumors treated with 3-dimensional partial tumor irradiation (LATTICE) had increased ASMase activity and were noted to inhibit growth of human umbilical vein endothelial cells.[38]

Immunomodulation

The interplay between radiation therapy and the immune system has been the subject of much research, especially with potential synergy with immunotherapy.[48] Generally, leukocytes are considered very vulnerable to radiation, and therefore radiation therapy is taken to be immunosuppressive.[49] However, studies have found an increase in tumor-infiltrating lymphocytes after radiation therapy in B16 melanoma in mice models, emphasizing the role of cellular immunity in maintaining tumor regression after radiation therapy.[50,51] Radiation therapy stimulated the activity of antigen-presenting cells, which in turn primed CD8+ T cells in draining lymph nodes.[50] The number of cytotoxic T cells infiltrating the irradiated tumor increased after radiation therapy, and, interestingly, it was noted that a single fraction of 15 Gy was more effective in this than 15 Gy over 3 fractions.[50] The addition of immunotherapy amplified the radiation-induced cytotoxic T cell response.[51] Consistent with the proposed role of cellular immunity, type 1 interferon was shown to be upregulated after radiation therapy and was necessary for T cell priming by dendritic cells.[52] In mice injected with murine mammary carcinoma into both flanks, cell-mediated tumor killing not only was limited to the irradiated tumor but also led to enhanced control of the distant site (ie, the abscopal effect).[53] Formenti et al[54] compared this to an in situ vaccine. This phenomenon has been further described as immunogenic cell death wherein dying tumors cells release tumor-associated antigens that stimulate antitumor immunity.[48,55]

In mice with implanted with xenograft A549 lung adenocarcinoma bilaterally, treating 1 tumor with SFRT reduced the growth of both tumors after 90 days.[27,48] The untreated tumor then also responded more than expected with 2 Gy fractionated radiation therapy. Kanagavelu et al[38] assessed the abscopal effects of LATTICE, a 3-dimensional form of grid in a murine model with allogenic bilateral Lewis lung carcinoma, by irradiating varying tumor volumes of 1 of the 2 tumors (Fig. 4).[38] They observed that (1) partial irradiation caused greater tumor growth delay in the distant nonirradiated tumor than did total irradiation and (2) irradiating two 10% volumes inhibited distant tumor growth more than did one 20% volume. There was induction of cytokines mediating cellular immunity, IL-2 and IFNg, whereas cytokines involved in humoral immunity, IL-4 and IL-10, were downregulated. In addition, there was increase in the number of infiltrating CD3+ T cells in both the irradiated site and the distant site. This correlated with the deceleration of tumor growth.[38]

Markovsky et al[56] recently reported the importance of CD8+ T cells and adhesion molecules, or ICAMs, in mediating tumor control in nonirradiated bystander areas. Using 67NR breast cancer cells implanted in mice, they found similar tumor growth delays whether 100% or 50% of the tumor volume was irradiated. Of note, this effect was abrogated if the mice were athymic, treated with antibodies against CD8+ cells, or treated with antibodies against ICAMs, demonstrating the CD8+ T cell dependency of the effect. Immunofluorescence confirmed an influx of primed CD8+ T cells within the nonirradiated part of the tumor. Further investigation revealed that early-infiltrating lymphocytes migrate from the surrounding tissue and the irradiated volume, whereas lymphocytes from lymph nodes maintained long-term antitumor activity. Markovsky et al also noted long-term immunomodulatory effects when reimplantation of 67NR breast cancer cells in these mice failed to produce another tumor.

Expanding the Concept of GRID

As described earlier, an immediately apparent problem with GRID therapy is its 2-dimensional nature: The effects of differential dose falloff from attenuation are not considered, and critical OARs beyond the target cannot be dose constrained. Newer modalities described in the following seek to address this fundamental limitation.

LATTICE (3-dimensional GRID)

Wu et al expanded the concept of SFRT into a 3-dimensional format: LRT.[57] By positioning multiple beams to converge at single high-dose spheres called vertices, LRT reduces the radiation absorbed by superficial normal tissue or OARs by limiting peak doses to within the GTV.[57,58] Delivery can be done with IMRT or aperture-modulated arc technique.[57] The radiobiological data were summarized earlier.[38]

Amendola et al[58] have the most clinical experience with LRT, treating more than 30 patients thus far. As reported in 3 separate case reports, they treated large tumors (cervical squamous cell carcinoma, ovarian carcinosarcoma, and non-small cell lung cancer, respectively) with excellent local control and minimal toxicity (Fig. 5).[58–60] Vertex sizes ranged from 1 to 2 cm

in diameter, and the distance between vertices ranged from 2 to 3 cm center to center. Notably, treatment schedules were different among the reports: a vertex dose of 48 Gy in 22 fractions of LRT,[59] a vertex dose 18 Gy in 1 fraction with conventional EBRT of 58 Gy in 29 fractions,[58] and a vertex dose of 27 Gy in 3 fractions of LRT with a motley of conventional EBRT, integrated boosts, and strips.[60] With differences between total doses and fractionation and the addition of other therapies, it is difficult to gain a sense of the effectiveness of LRT. Moreover, although the vertices were configured to avoided OARs, it is unclear if there was a systematic approach for treatment planning.[58]

Microbeam radiation therapy

Microbeam radiation therapy (MRT) is a form of spatial fractionation using beams the size of microns, with widths of 25 to 50 microns and spacing around 200 to 400 microns.[61] Remarkably, this allows peak doses as high as 100 Gy while sparing the majority of normal tissue. As many propose, such effects present a huge opportunity for brain cancers, in particular glioblastoma multiforme in adults and diffuse pontine infiltrating glioma in children.[62] Preclinical data remarkably support the effectiveness of MRT; yet many technical and logistical challenges remain, preventing the transition to clinical trials.[63] Excellent reviews are available on MRT for further reading.[61,62]

Proton GRID

Protons have the advantage of reaching their maximum dose at the Bragg peak with low entrance dose and no exit dose, in stark contrast to photons in standard GRID (Fig. 6).[64] Using the technical capabilities afforded by pencil-beam scanning, Henry et al[65] first suggested SFRT using protons. Simulation studies demonstrated the feasibility of delivering proton SFRT therapy with interlaced crossfiring millimeter-sized beams in fairly homogenous dose distributions.[66,67] In contrast, Gao et al[68] mimicked a photon SFRT with 1-cm apertures and 2-cm center-to-center spacing at isocenter in a hexagonal pattern and observed a dose profile in which the maximum proton doses remain within the tumor and a steep dropoff at the end with similar valley-to-peak dose ratios to photons at various depths.[68] Two patients treated by Gao et al with proton SFRT to avoid critical structures tolerated the treatment with only grade 1 dermatitis.[68] Clinical data are otherwise limited. Taking inspiration from photon minibeam radiation therapy, dosimetric and preclinical data are emerging on the feasibility of proton minibeam.[69–74]

Considerations for Future Research

On August 21, 2018, a workshop held by the National Cancer Institute and the Radiosurgery Society reviewed the proposed radiobiological mechanisms and existing clinical data on SFRT, emphasizing areas for further research. The group identified a need for guidelines and standards for institutions to incorporate SFRT, addressing the need to standardize appropriate SFRT peak-valley dose and center-to-center spacing, the interval of SFRT fractions if more than 1 fraction is planned, the scheduling and sequencing of SFRT and conventional EBRT combinations, and more. Further biological experiments using animal models as well as phase 1 and 2 trials are essential to clarify optimal dosing and regimens.

In addition, preclinical data are urgently needed to parameterize and model the radiobiological sequelae of changing aperture sizes, center-to-center spacing, and hole patterns. It is equally important that the dosimetry of SFRT can be reliably validated. Biomarkers, including the tumor, serum, and other signaling molecules mentioned earlier, should be measured to correlate with radiobiological data. Clinical studies thus far have not assessed for long-term toxicities. It has been argued that overall survival should be the most relevant endpoint, not local control.

A query of clinical trials registered with the National Institutes of Health using the search term “GRID radiotherapy” identified a phase 1 trial observing the toxicity of GRID in pediatric osteosarcoma (ClinicalTrials.gov Identifier: NCT03139318); a phase 2 study evaluating palliative outcomes in radioresistant or bulky tumors (NCT02333110); and a radiobiological trial assessing the effects of GRID on interstitial fluid pressure and tumor oxygenation (NCT01967927). A second query using “lattice radiotherapy” identified an active early-phase clinical trial (NCT01411319) assessing the safety of a single fraction of lattice before conventional EBRT in treating prostate cancer and the effect on tumor biomarkers and a second recruiting clinical trial (NCT02307058) comparing lattice and conventional EBRT against a moderately hypofractionated regimen.

Conclusion

SFRT delivers high doses of radiation without exceeding the tolerance of critical structures, particularly skin, by limiting the volume of irradiated tissue. Early-phase clinical studies show excellent response rates, often with dramatic and rapid resolution of large tumors. Technological advancements continue to expand its use into unique and more reproducible formats. Radiobiological experiments support the role of radiation-induced bystander effects, vascular alterations, and immunologic interactions. However, further preclinical data are necessary to determine optimal SFRT planning, and clinical trials need to clearly define the role of SFRT in the clinical setting.

References

1. Laissue J, Blattmann H, Slatkin D. [Alban Köhler (1874-1947): Inventor of grid therapy]. Z Med Phys 2012;22:90–99. [PubMed: 21862299]
2. Liberson F The value of a multi-perforated screen in deep X-ray therapy: A preliminary report on a new method of delivering multiple erythema doses without permanent injury to the skin. Radiology 1933;20:186–195.
3. Marks H Clinical experience with irradiation through a grid. Radiology 1952;58:338–342. [PubMed: 14900413]
4. Failla G Irradiation through grids. Radiology 1952;58:424–426.
5. Mohiuddin M, Curtis DL, Grizos WT, Komarnicky L. Palliative treatment of advanced cancer using multiple nonconfluent pencil beam radiation. A pilot study. Cancer 1990;66:114–118. [PubMed: 1693874]
6. Dubben HH, Thames HD, Beck-Bornholdt HP. Tumor volume: A basic and specific response predictor in radiotherapy. Radiother Oncol 1998;47:167–174. [PubMed: 9683365]
7. Mohiuddin M, Stevens JH, Reiff JE, Huq MS, Suntharalingam N. Spatially fractionated (GRID) radiation for palliative treatment of advanced cancer. Radiation Oncology Investigations 1996;4:41–47.

8. Reiff JE, Saiful Huq M, Mohiuddin M, Suntharalingam N. Dosimetric properties of megavoltage grid therapy. Int J Radiat Biol Phys 1995;33:937–942.
9. Gholami S, Nedaie HA, Longo F, Ay MR, Dini SA, Meigooni AS. Grid block design based on Monte Carlo simulated dosimetry, the linear quadratic and Hug-Kellerer radiobiological models. J Med Phys 2017;42:213–221. [PubMed: 29296035]
10. Meigooni AS, Dou K, Meigooni NJ, et al. Dosimetric characteristics of a newly designed grid block for megavoltage photon radiation and its therapeutic advantage using a linear quadratic model. Med Phys 2006;33:3165–3173. [PubMed: 17022209]
11. Buckey C, Stathakis S, Cashon K, et al. Evaluation of a commercially-available block for spatially fractionated radiation therapy. J Appl Clin Med Phys 2010;11:3163. [PubMed: 20717082]
12. Ha JK, Zhang G, Naqvi SA, Regine WF, Yu CX. Feasibility of delivering grid therapy using a multileaf collimator. Med Phys 2006; 33:76–82. [PubMed: 16485412]
13. Neuner G, Mohiuddin MM, Vander Walde N, et al. High-dose spatially fractionated GRID radiation therapy (SFGRT): A comparison of treatment outcomes with Cerrobend vs. MLC SFGRT. Int J Radiat Oncol Biol Phys 2012;82:1642–1649. [PubMed: 21531514]
14. Nobah A, Mohiuddin M, Devic S, Moftah B. Effective spatially fractionated GRID radiation treatment planning for a passive grid block. Br J Radiol 2015;88:20140363. [PubMed: 25382164]
15. Almendral P, Mancha PJ, Roberto D. Feasibility of a simple method of hybrid collimation for megavoltage grid therapy. Med Phys 2013; 40:051712. [PubMed: 23635260]
16. Zhang X, Penagaricano J, Yan Y, et al. Application of spatially fractionated radiation (GRID) to helical tomotherapy using a novel TOMOGRID template. Technol Cancer Res Treat 2016;15: 91–100. [PubMed: 24000988]
17. Gholami S, Severgnini M, Nedaie HA, Longo F, Meigooni AS. PO-0947: VMAT-based grid for spatially fractionated radiation therapy. Radiother Oncol 2016;119:S460.
18. Mohiuddin M, Fujita M, Regine WF, Megooni AS, Ibbott GS, Ahmed MM. High-dose spatially-fractionated radiation (GRID): A new paradigm in the management of advanced cancers. Int J Radiat Oncol Biol Phys 1999;45:721–727. [PubMed: 10524428]
19. Kudrimoti M, Regine WF, Huhn JL, Meigooni AS, Ahmed M, Mohiuddin M. Spatially fractionated radiation therapy (SFR) in the palliation of large bulky (>8 cm) melanomas. Int J Radiat Biol Phys 2002;54:342–343.
20. Mohiuddin M, Miller T, Ronjon P, Malik U. Spatially fractionated grid radiation (SFGRT): A novel approach in the management of recurrent and unresectable soft tissue sarcoma. Int J Radiat Oncol Biol Phys 2009;75:S526.
21. Mohiuddin M, Memon M, Nobah A, et al. Locally advanced high-grade extremity soft tissue sarcoma: Response with novel approach to neoadjuvant chemoradiation using induction spatially fractionated GRID radiotherapy (SFGRT). J Clin Oncol 2014;32: 10575; 10575.
22. Huhn JL, Regine WF, Valentino JP, Meigooni AS, Kudrimoti M, Mohiuddin M. Spatially fractionated GRID radiation treatment of advanced neck disease associated with head and neck cancer. Technol Cancer Res Treat 2006;5:607–612. [PubMed: 17121437]
23. Penagaricano JA, Moros EG, Ratanatharathorn V, Yan Y, Corry P. Evaluation of spatially fractionated radiotherapy (GRID) and definitive chemoradiotherapy with curative intent for locally advanced squamous cell carcinoma of the head and neck: Initial response rates and toxicity. Int J Radiat Oncol Biol Phys 2010;76: 1369–1375. [PubMed: 19625138]
24. Edwards JM, Shah PH, Huhn JL, et al. Definitive GRID and fractionated radiation in bulky head and neck cancer associated with low rates of distant metastasis. Int J Radiat Oncol Biol Phys 2015;93: E334.
25. Mohiuddin M, Park H, Hallmeyer S, Richards J. High-dose radiation as a dramatic, immunological primer in locally advanced melanoma. Cureus 2015;7:e417. [PubMed: 26848410]
26. Kaiser A, Mohiuddin MM, Jackson GL. Dramatic response from neoadjuvant, spatially fractionated GRID radiotherapy (SFGRT) for large, high-grade extremity sarcoma. J Radiat Oncol 2012;2:103–106.
27. Prasanna A, Ahmed MM, Mohiuddin M, Coleman CN. Exploiting sensitization windows of opportunity in hyper and hypo-fractionated radiation therapy. J Thorac Dis 2014;6:287–302. [PubMed: 24688774]

28. Hopewell JW, Trott KR. Volume effects in radiobiology as applied to radiotherapy. Radiother Oncol 2000;56:283–288. [PubMed: 10974376]
29. Blyth BJ, Sykes PJ. Radiation-induced bystander effects: What are they, and how relevant are they to human radiation exposures? Radiat Res 2011;176:139–157. [PubMed: 21631286]
30. Emerit I, Levy A, Cernjavski L, et al. Transferable clastogenic activity in plasma from persons exposed as salvage personnel of the Chernobyl reactor. J Cancer Res Clin Oncol 1994;120:558–561. [PubMed: 8045922]
31. Lyng FM, Seymour CB, Mothersill C. Production of a signal by irradiated cells which leads to a response in unirradiated cells characteristic of initiation of apoptosis. Br J Cancer 2000;83:1223–1230. [PubMed: 11027437]
32. Azzam EI, de Toledo SM, Little JB. Oxidative metabolism, gap junctions and the ionizing radiation-induced bystander effect. Oncogene 2003;22:7050. [PubMed: 14557810]
33. Prise KM, O'Sullivan JM. Radiation-induced bystander signalling in cancer therapy. Nat Rev Cancer 2009;9:351–360. [PubMed: 19377507]
34. Najafi M, Fardid R, Hadadi G, Fardid M. The mechanisms of radiation-induced bystander effect. J Biomed Phys Eng 2014;4: 163–172. [PubMed: 25599062]
35. Asur RS, Sharma S, Chang CW, et al. Spatially fractionated radiation induces cytotoxicity and changes in gene expression in bystander and radiation adjacent murine carcinoma cells. Radiat Res 2012;177: 751–765. [PubMed: 22559204]
36. Sathishkumar S, Dey S, Meigooni AS, et al. The impact of TNF-alpha induction on therapeutic efficacy following high dose spatially fractionated (GRID) radiation. Technol Cancer Res Treat 2002;1:141–147. [PubMed: 12622521]
37. Shareef MM, Cui N, Burikhanov R, et al. Role of tumor necrosis factor-alpha and TRAIL in high-dose radiation-induced bystander signaling in lung adenocarcinoma. Cancer Res 2007;67: 11811–11820. [PubMed: 18089811]
38. Kanagavelu S, Gupta S, Wu X, et al. In vivo effects of lattice radiation therapy on local and distant lung cancer: Potential role of immunomodulation. Radiat Res 2014;182:149–162. [PubMed: 25036982]
39. Folkman J Role of angiogenesis in tumor growth and metastasis. Semin Oncol 2002;29(6 Suppl 16):15–18.
40. Haimovitz-Friedman A, Kan CC, Ehleiter D, et al. Ionizing radiation acts on cellular membranes to generate ceramide and initiate apoptosis. J Exp Med 1994;180:525–535. [PubMed: 8046331]
41. Santana P, Pena LA, Haimovitz-Friedman A, et al. Acid sphingomyelinase-deficient human lymphoblasts and mice are defective in radiation-induced apoptosis. Cell 1996;86:189–199. [PubMed: 8706124]
42. Garcia-Barros M, Paris F, Cordon-Cardo C, et al. Tumor response to radiotherapy regulated by endothelial cell apoptosis. Science 2003; 300:1155–1159. [PubMed: 12750523]
43. Garcia-Barros M, Lacorazza D, Petrie H, et al. Host acid sphingomyelinase regulates microvascular function not tumor immunity. Cancer Res 2004;64:8285–8291. [PubMed: 15548696]
44. Alphonse G, Bionda C, Aloy MT, Ardail D, Rousson R, Rodriguez-Lafrasse C. Overcoming resistance to γ-rays in squamous carcinoma cells by poly-drug elevation of ceramide levels. Oncogene 2004;23:2703. [PubMed: 15048093]
45. Hara S, Nakashima S, Kiyono T, et al. p53-Independent ceramide formation in human glioma cells during gamma-radiation-induced apoptosis. Cell Death Differ 2004;11:853–861. [PubMed: 15088070]
46. Sathishkumar S, Boyanovsky B, Karakashian AA, et al. Elevated sphingomyelinase activity and ceramide concentration in serum of patients undergoing high dose spatially fractionated radiation treatment: Implications for endothelial apoptosis. Cancer Biol Ther 2005;4:979–986. [PubMed: 16096366]
47. Nolan MW, Gieger TL, Karakashian AA, et al. Outcomes of spatially fractionated radiotherapy (GRID) for bulky soft tissue sarcomas in a large animal model. Technol Cancer Res Treat 2017;16:357–365. [PubMed: 28168937]

48. Wattenberg MM, Fahim A, Ahmed MM, Hodge JW. Unlocking the combination: Potentiation of radiation-induced antitumor responses with immunotherapy. Radiat Res 2014;182:126–138. [PubMed: 24960415]
49. Manda K, Glasow A, Paape D, Hildebrandt G. Effects of ionizing radiation on the immune system with special emphasis on the interaction of dendritic and T cells. Front Oncol 2012;2:102. [PubMed: 22937525]
50. Lugade AA, Moran JP, Gerber SA, Rose RC, Frelinger JG, Lord EM. Local radiation therapy of B16 melanoma tumors increases the generation of tumor antigen-specific effector cells that traffic to the tumor. J Immunol 2005;174:7516. [PubMed: 15944250]
51. Lee Y, Auh SL, Wang Y, et al. Therapeutic effects of ablative radiation on local tumor require CD8+ T cells: Changing strategies for cancer treatment. Blood 2009;114:589–595. [PubMed: 19349616]
52. Burnette BC, Liang H, Lee Y, et al. The efficacy of radiotherapy relies upon induction of type i interferon-dependent innate and adaptive immunity. Cancer Res 2011;71:2488–2496. [PubMed: 21300764]
53. Demaria S, Ng B, Devitt ML, et al. Ionizing radiation inhibition of distant untreated tumors (abscopal effect) is immune mediated. Int J Radiat Oncol Biol Phys 2004;58:862–870. [PubMed: 14967443]
54. Formenti SC, Demaria S. Radiotherapy to convert the tumor into an in situ vaccine. Int J Radiat Oncol Biol Phys 2012;84:879–880. [PubMed: 23078897]
55. Hannani D, Sistigu A, Kepp O, Galluzzi L, Kroemer G, Zitvogel L. Prerequisites for the antitumor vaccine-like effect of chemotherapy and radiotherapy. Cancer J 2011;17:351–358. [PubMed: 21952286]
56. Markovsky E, Budhu S, Samstein RM, et al. An anti-tumor immune response is evoked by partial-volume single dose radiation in two murine models. Int J Radiat Biol Phys 2019;103:697–708.
57. Wu X, Ahmed MM, Wright J, Gupta S, Pollack A. On modern technical approaches of three-dimensional high-dose lattice radiotherapy (LRT). Cureus 2018;2:e9.
58. Amendola BE, Perez NC, Wu X, Blanco Suarez JM, Lu JJ, Amendola M. Improved outcome of treating locally advanced lung cancer with the use of lattice radiotherapy (LRT): A case report. Clin Transl Radiat Oncol 2018;9:68–71. [PubMed: 29594253]
59. Amendola BE, Perez N, Amendola MA, et al. Lattice radiotherapy with RapidArc for treatment of gynecological tumors: Dosimetric and early clinical evaluations. Cureus 2010;2:e15.
60. Blanco Suarez JM, Amendola BE, Perez N, Amendola M, Wu X. The use of lattice radiation therapy (LRT) in the treatment of bulky tumors: A case report of a large metastatic mixed Mullerian ovarian tumor. Cureus 2015;7:e389. [PubMed: 26719832]
61. Grotzer MA, Schultke E, Brauer-Krisch E, Laissue JA. Microbeam radiation therapy: Clinical perspectives. Phys Med 2015;31:564–567. [PubMed: 25773883]
62. Schültke E, Balosso J, Breslin T, et al. Microbeam radiation therapy — grid therapy and beyond: A clinical perspective. Br J Radiol 2017; 90:20170073. [PubMed: 28749174]
63. Wright MD. Microbeam radiosurgery: An industrial perspective. Physica Medica 2015;31:601–606. [PubMed: 25937007]
64. Newhauser WD, Zhang R. The physics of proton therapy. Phys Med Biol 2015;60:R155–R209. [PubMed: 25803097]
65. Henry T, Ureba A, Valdman A, Siegbahn A. Proton grid therapy. Technol Cancer Res Treat 2016;16 1533034616681670.
66. Henry T, Valdman A, Siegbahn A. OC-0546: The development of proton-beam grid therapy (PBGT). Radiother Oncol 2016;119: S260–S261.
67. Henry T, Bassler N, Ureba A, Tsubouchi T, Valdman A, Siegbahn A. Development of an interlaced-crossfiring geometry for proton grid therapy. Acta Oncol 2017;56:1437–1443. [PubMed: 28826311]
68. Gao M, Mohiuddin MM, Hartsell WF, Pankuch M. Spatially fractionated (GRID) radiation therapy using proton pencil beam scanning (PBS): A feasibility study. Int J Radiat Oncol Biol Phys 2015;93:E562; E562.

69. Prezado Y, Fois GR. Proton-minibeam radiation therapy: A proof of concept. Med Phys 2013;40:031712. [PubMed: 23464307]

70. Dilmanian FA, Eley JG, Krishnan S. Minibeam therapy with protons and light ions: Physical feasibility and potential to reduce radiation side effects and to facilitate hypofractionation. Int J Radiat Oncol Biol Phys 2015;92:469–474. [PubMed: 25771360]

71. Peucelle C, Nauraye C, Patriarca A, et al. Proton minibeam radiation therapy: Experimental dosimetry evaluation. Med Phys 2015;42: 7108–7113. [PubMed: 26632064]

72. Girst S, Greubel C, Reindl J, et al. Proton minibeam radiation therapy reduces side effects in an in vivo mouse ear model. Int J Radiat Biol Phys 2016;95:234–241.

73. Prezado Y, Jouvion G, Hardy D, et al. Proton minibeam radiation therapy spares normal rat brain: Long-term clinical, radiological and histopathological analysis. Scientific Reports 2017;7:14403. [PubMed: 29089533]

74. Sammer M, Greubel C, Girst S, Dollinger G. Optimization of beam arrangements in proton minibeam radiotherapy by cell survival simulations. Med Phys 2017;44:6096–6104. [PubMed: 28880369]

75. Martinez-Rovira I, Fois G, Prezado Y. Dosimetric evaluation of new approaches in GRID therapy using nonconventional radiation sources. Med Phys 2015;42:685–693. [PubMed: 25652482]

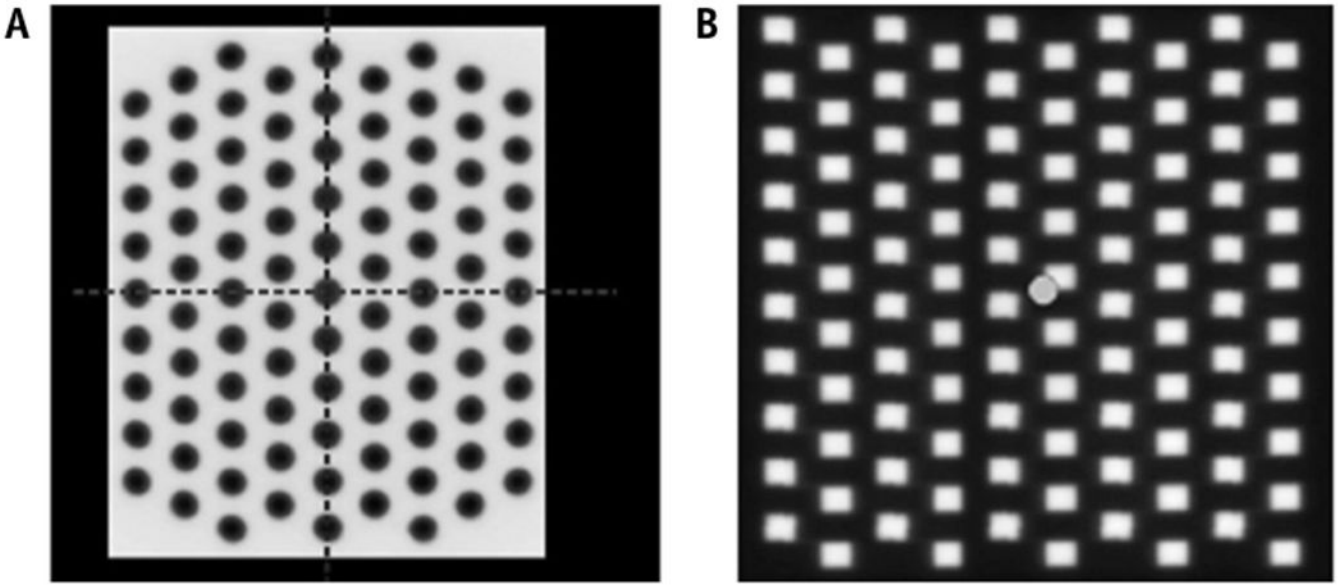

Fig. 1.
Representative GRID patterns created by a (A) Cerrobend block or (B) multileaf collimators, reproduced with permission from Neuner et al.[13]

Fig. 2.

(A) Taken with permission from Mohiuddin et al,[25] a patient with an uncontrolled 18-cm nodal melanoma mass, progressing after IL-2, ipilumimab, and pembrolizumab. The authors treated with 20-Gy SFRT followed by 50-Gy conventional EBRT and pembrolizumab with a complete and sustained response. (B) Taken with permission from Kaiser et al,[26] a rapidly progressing upper extremity spindle cell sarcoma despite conventional EBRT was treated with 18-Gy GRID boosted by 32-Gy EBRT. Tumor regression was 90%, including gross tumor involving the medial humerus that was shielded. *Abbreviations:* EBRT = external beam radiation therapy; SFRT = spatially fractionated radiation therapy.

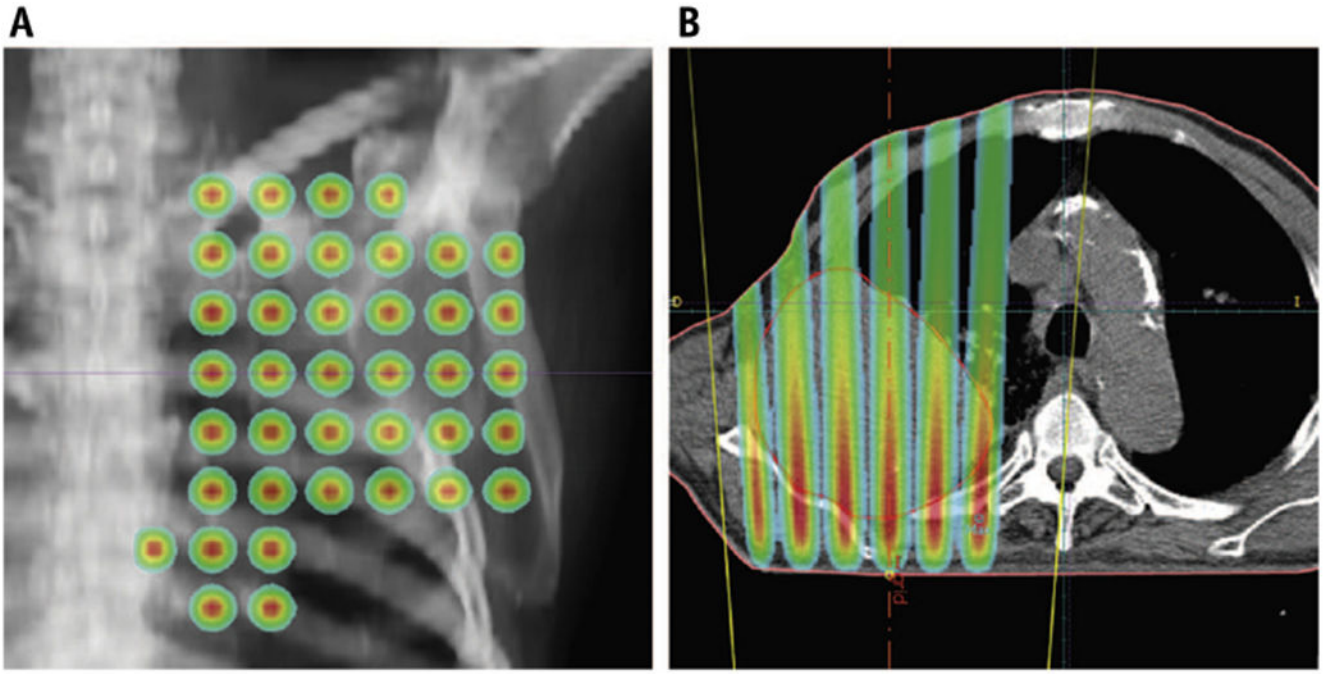

Fig. 3.

Treatment planning of a patient with lung cancer, reproduced with permission from Almendral et al.[15] (A) Anteroposterior view. (B) Transverse view. The nonuniform dose distribution peaks at entry near the skin and attenuates as it approaches the anterior aspects of the tumor.

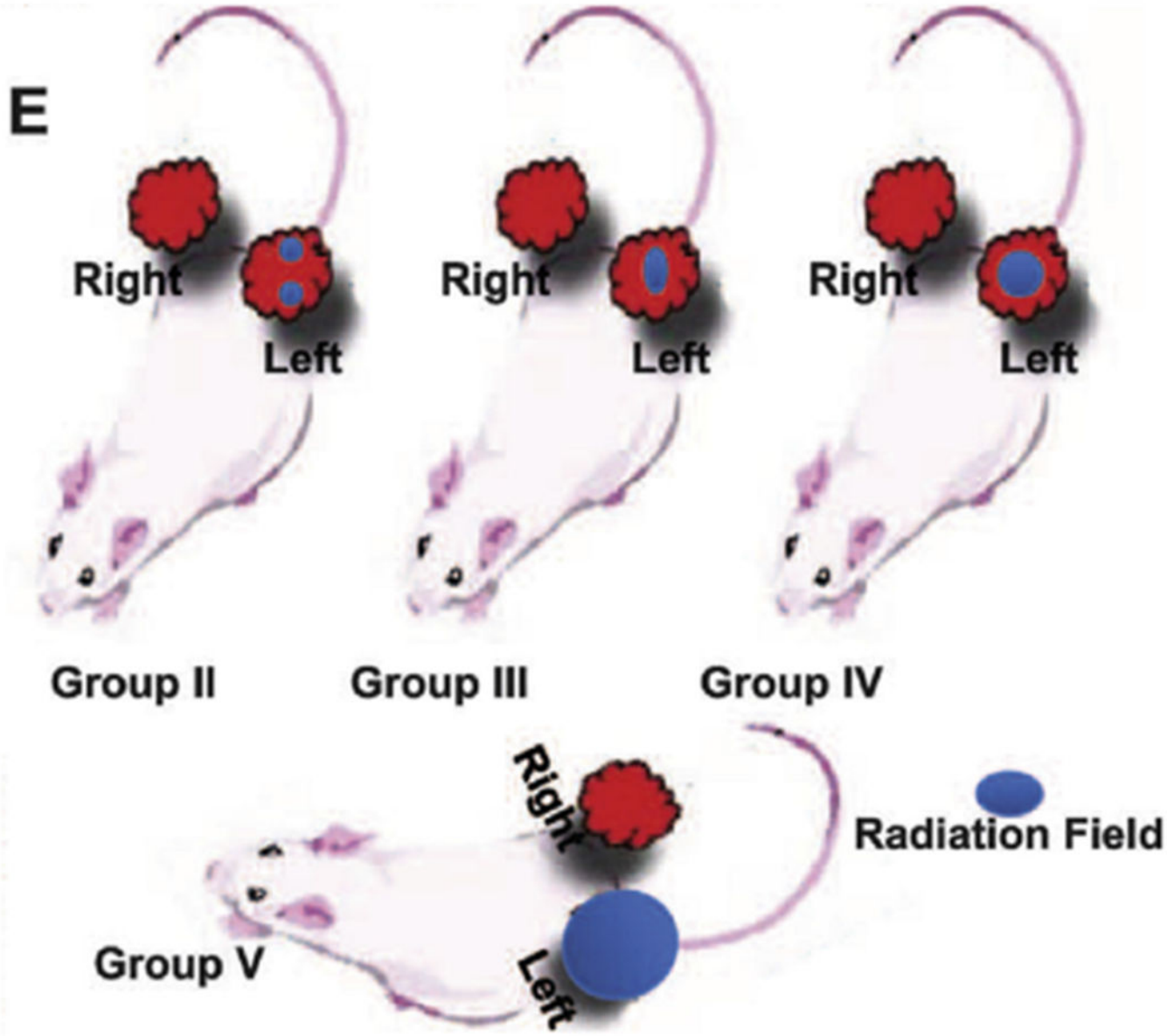

Fig. 4.

Taken with permission from Kanagavelu et al[38] (© 2019 Radiation Research Society), cartoon depiction of 3 radiotherapy conditions. Group II, with two 10% irradiated volumes, had better ipsilateral and contralateral tumor control.

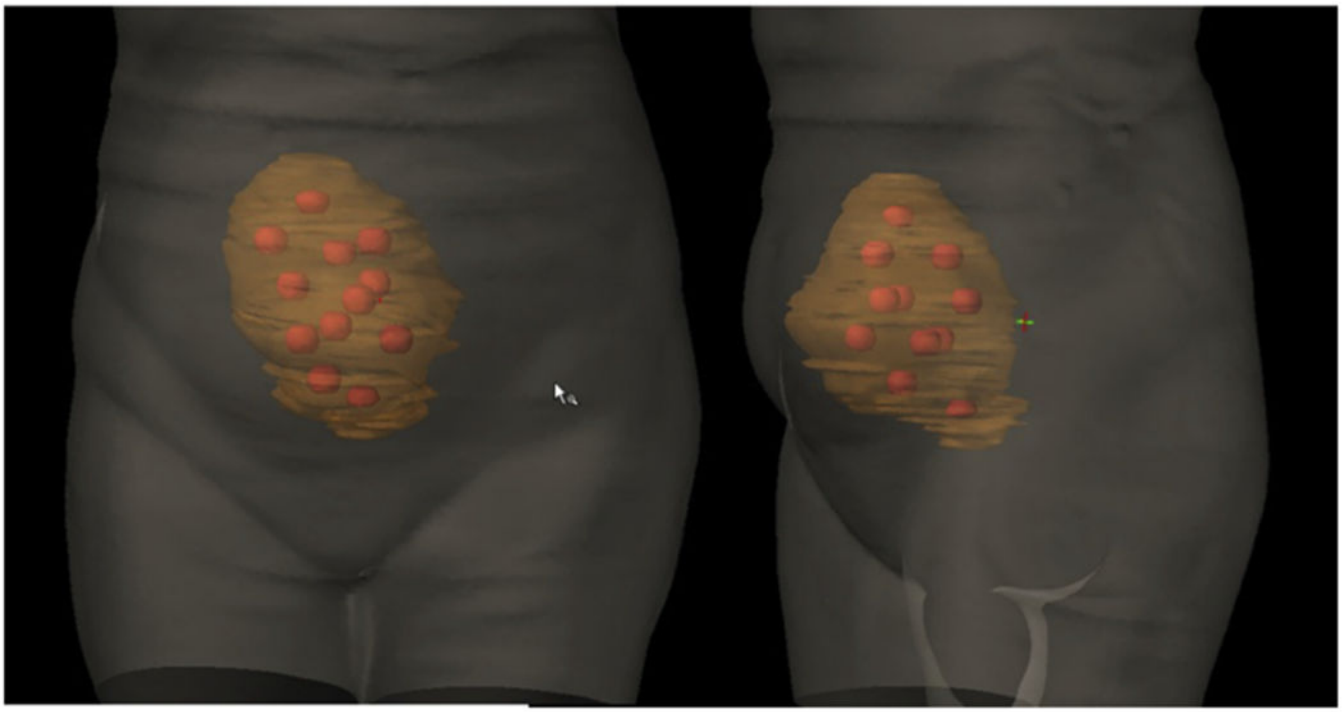

Fig. 5.

Lattice radiation therapy treatment plan of bulky ovarian tumor involves creating high-dose spheres distributed within the 3-dimensional tumor volume, reproduced with permission from Blanco-Suarez et al.[60]

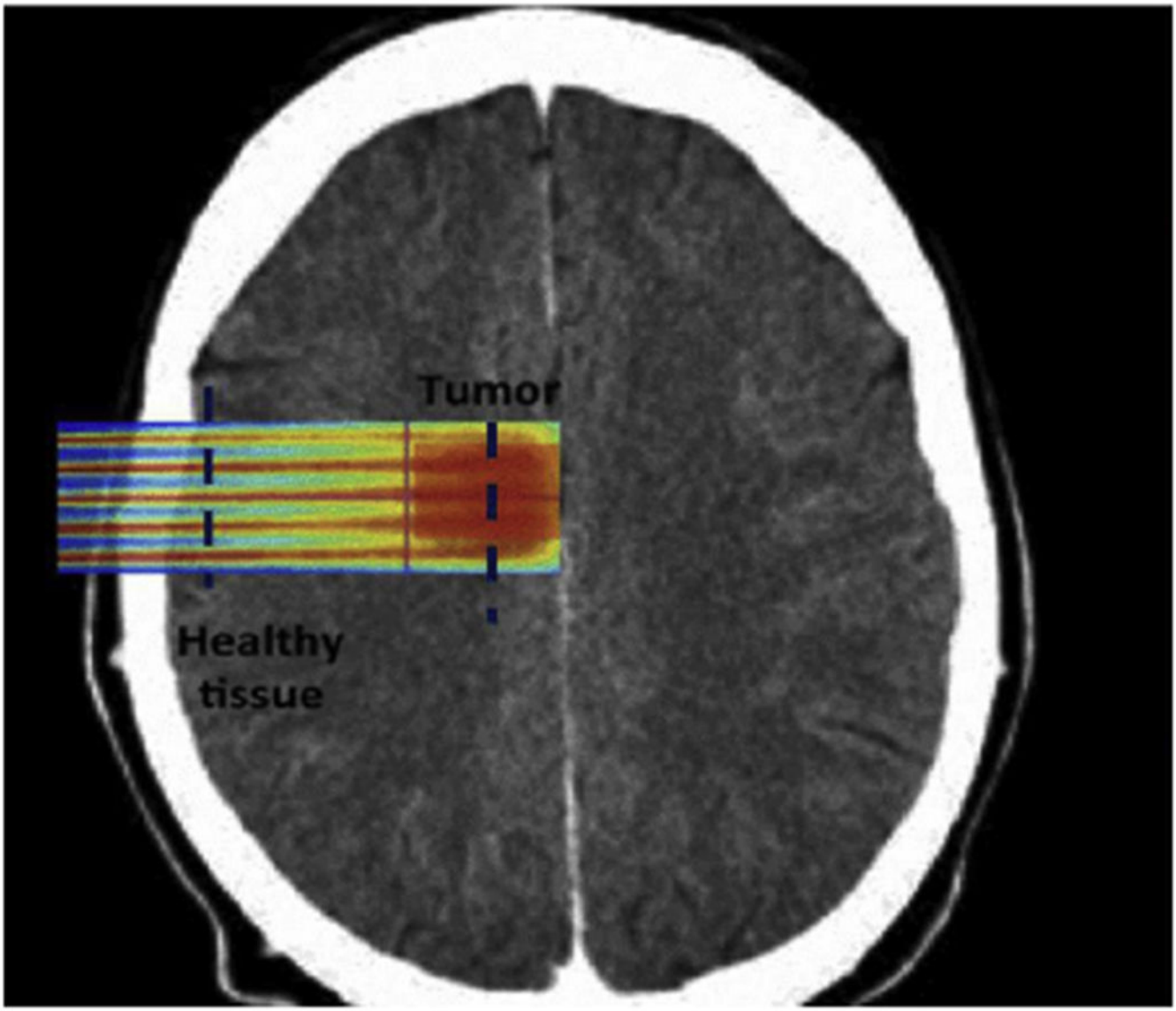

Fig. 6.

Treatment planning for a brain tumor, reproduced with permission from Martinez-Rovira et al.[75] Proton GRID allows for more precise dosing to spare normal tissue in sensitive organs at risk.

Table 1

Comparison of technologies used to create GRID dosimetry

	Pros	Cons
Collimator block	• Cost-effective • Reusable • Can be customized to specifications • Adjustable field by closing jaws	• Made to order • Limited to 1 pattern • Heavy • Necessary to mount and dismount
Multileaf collimator	• Available in most institutions • More flexible in creating field pattern	• Long delivery time • Requires more monitor units • More radiation leakage • Higher valley-to-peak doses • Higher surface doses
Hybrid collimation	• Easier to craft • Lighter than block • Faster than multileaf collimator	• Valley-to-peak ratio lower along diagonals

Table 2

Summary of clinical studies

Authors	Treated Sites (n)	Follow-up, median (range) (mo)	Histology	GRID dose, median (range) (Gy)	Prior RT	GRID only	Control rates	Side effects
Mohiuddin et al, 1990[5]	22	NR (1-18)	Diverse	NR (10-15)	27%	36%	Response rate: 91%	1 acute skin erythema, 2 N&V, 2 diarrhea, 1 late SBO
Mohiuddin et al, 1996[7]	72	4 (0.5-28)	Diverse	NR (10-25)	24%	44%	Response rate: 91%	No grade 2 or higher acute toxicity
Mohiuddin et al, 1999[18]	87	7 (3-42)	Diverse	15 (10-20)	9%	20%	Response rate: 91%	1 grade 3 acute mucositis, 1 fatal carotid blowout
Kudrimoti et al, 2002[19]	20	NR	Melanoma	15 (12-20)	25%	25%	Response rate: 80%	No grade 3 or higher toxicities
Huhn et al, 2006[22]	27	10 (3-44)	SCC of H&N	15 (15-20)	0%	0%	(1) Neck control rate: 93%; (2) neck control rate 92%	(1) acute G 2-3 skin toxicity, 10 late G 2 soft tissue and muscle fibrosis; (2) 3 poor postoperative wound healing, 4 fibrosis limiting neck movement
Mohiuddin et al, 2009[20]	44	9 (2-44)	Soft tissue sarcoma	15 (12-20)	NR	9%	Response rate 76%	2 G 3 acute skin reactions
Penagaricano et al, 2010[23]	14	19.5 (2-38)	SCC of H&N	20	0%	0%	Local control rate: 79%	1 fatal carotid blowout, 11 acute G 2-3 skin reaction, 13 acute G 2-3 mucosal reaction, 4 late G 2-3 skin fibrosis
Neuner et al, 2012[13]	79	2 (0-51.6)	Diverse	15 (10-20)	NR	20%	Pain response rate, block: 95%, pain response rate, MLC: 74%, mass effect response rate, block: 84%, mass effect response rate, MLC: 79%	4 G 3-4 acute skin reactions with block versus 10 G 3-4 acute skin reactions with MLC
Mohiuddin et al, 2014[21]	14	14 (3-43)	Soft tissue sarcoma	18	0%	0%	Local control rate: 100%	1 G 3 acute skin, 2 delayed wound healing
Edwards et al, 2015[24]	53	mean 34 (1-239)	SCC of H&N	15	NR	0%	Local control rate: 81%	2 late toxicities requiring feeding tubes

Abbreviations: G = grade; H&N = head and neck; MLC = multileaf collimator; N&V = nausea and vomiting; NR = not reported; RT = radiation therapy; SCC = squamous cell carcinoma.